metals

MDPI

Article

The Effect of Strain on the Formation of an Intermetallic Layer in an Al-Ni Laminated Composite

Monireh Azimi [1,2], Mohammad Reza Toroghinejad [1], Morteza Shamanian [1] and Leo A. I. Kestens [2,3,*]

1 Department of Materials Engineering, Isfahan University of Technology, Isfahan 84156-83111, Iran; Monireh.Azimi@UGent.be (M.A.); toroghi@cc.iut.ac.ir (M.R.T.); shamanian@cc.iut.ac.ir (M.S.)
2 Metal Science and Technology Group, EEMMeCS Department, Ghent University, Technologiepark 903, 9052 Ghent, Belgium
3 Materials Science and Technology Department, Delft University of Technology, Mekelweg 2, 2628 CD Delft, The Netherlands
* Correspondence: Leo.Kestens@UGent.be; Tel.: +32-475-342-010

Received: 5 September 2017; Accepted: 16 October 2017; Published: 20 October 2017

Abstract: In the present work, the influence of strain on phase formation at the Al/Ni interface was investigated during cold roll bonding and annealing. A sandwich sample composed of an Al-Ni-Al stack was cold rolled with reductions in the range of 50% to 90%, followed by annealing at 450 °C for 60 min. The crystallography of the annealed sandwich samples was analyzed by XRD (X-ray diffraction), whereas the microstructure was studied by scanning electron microscopy, equipped with EDS (energy dispersive spectrometer) analysis, and optical microscope. In the annealed samples, the intermetallic phase Al_3Ni has formed at the Ni/Al interface, preferentially on the Al side of the interface. It is found that the applied strains did not have an effect on the type of intermetallic phase that was formed. However, the rolling reduction has a significant effect on the morphology of the intermetallic layer, as it was observed that after the lowest reduction of 50% only some scattered intermetallic nuclei were present, whereas at the highest rolling reduction of 90% a continuous intermetallic layer of 4.1 μm was exhibited. The formation of the intermetallic layer is discussed in terms of Al and Ni diffusion at the interface and irregular nature of the Al/Ni bonded interface after rolling reductions.

Keywords: aluminum; diffusion; intermetallic; laminated composite; nickel; roll bonding; strain

1. Introduction

Laminated metal composites are a unique form of composite in which alternating metals or metal-containing layers are bonded together [1]. Currently, there is a great interest in metal-intermetallic laminate (MIL) composites, because MIL composites have the potential to combine various functions, which may be of use for high-temperature structural applications such as heat exchangers, which require appropriate thermal management [1,2]. In the fabrication of these composites, high strength intermetallic reinforcement is used, while its low toughness is compensated for by the soft matrix.

Previous reports [1,3–9] have revealed that these materials can be produced by various manufacturing techniques, which can be categorized in the two main groups of deposition and bonding. Deposition techniques such as electrodeposition, evaporation, and sputtering involve atomic scale transport of the component materials. As-received MIL composites of this category conventionally exhibit nanostructures with extremely high strength. Deposition techniques require expensive equipment and complex processes, and thus they are slow and costly. This makes them difficult to be up-scaled to large, commercially viable production facilities. Bonding processes like

diffusion bonding, transient liquid phase bonding, and reaction bonding are relatively simple. There is usually no limitation in the size and number of component layers, and the process can be carried out even in atmospheric conditions.

A wide variety of MIL composites has been developed, including Al-Fe [10,11], Al-Ni [12–14], Al-Ti [15–18], Al-Cu [19–21], and Al-Mg [22,23] systems. Among them, intermetallic compounds of the Al-Ni system and their MIL composites are appropriate for use in aerospace, automotive and medical applications as structural materials. Such materials comply with functional demands such as lightweight, high thermal stability, fatigue resistance, creep and corrosion resistance at elevated temperatures and suitable ductility [7,24].

The determination of the type of Al-Ni intermetallic compounds in the laminated composite is of crucial importance for the ensuing thermal and mechanical properties of the composite. The sequence of phase formation has been previously studied and it was concluded that this sequence was controlled by both thermodynamics of the alloy system and the kinetics of the reaction process [24]. The latter factor is more influential in the early stages of the phase reaction, whereby kinetics is of crucial importance for the selection of phases in the early stages of the intermetallic compound formation. Such a phase selection can be caused by differences in nucleation rate as well as by differences in the growth rate of the competing phases.

It is noteworthy that some reports [25,26] indicated that concentration gradients and intermixing of constituents prior to phase transformation play a key role in the determination of phase formation kinetics. Different phase formation sequences have been reported for various nominal compositions and manufacturing processes [2,7,14,27–29]. However, in most cases, the Al_3Ni phase with an ordered $D0_{20}$ structure is formed first. But alternatively, initial intermediate phases such as Al-Ni, $AlNi_3$, or the metastable Al_9Ni_2 phase have also been observed during the manufacturing process, whereby the formation depends on the nominal composition of multilayers and the process history. Nevertheless, Sauvage et al. [27] confirmed that the first intermetallic phase formation was not dependant on the initial chemical composition of layers or the concentration gradient. They applied a repeated folding and rolling (F&R) process on Al-Ni multilayers to investigate phase formation kinetics at the atomic scale using 3D-atom probe analysis. It was understood that severe plastic deformation forced the constituents to intermix, whereby metastable or non-equilibrium Al and Ni solid solutions with various compositions were formed prior to annealing. These solid solutions constitute a diffuse interface between the Ni and Al laminates. During annealing, the Al_3Ni phase nucleated from such diffuse interfaces faster than in the deposition multilayers with sharp interfaces. Consequently, intermetallic compound Al_3Ni was recognized as a strongly favored intermetallic phase. Even the largely different chemical composition of the intermixed regions did not result in the formation of other phases. Additionally, researchers have reported conflicting Al and Ni asymmetric interdiffusion coefficient results, even under similar process conditions [2,27].

In most previous studies, hot or cold rolling and pressing, accumulative roll bonding (ARB), and F&R followed by annealing were applied to produce MIL composites in Al-M systems [1,2,7,14,18,20,22,23,27,30–34]. However, there is little published information on how the applied strain during the process affects the formation of intermetallic phases. Therefore, in the present study, this question was addressed by applying a cold roll bonding (CRB) process and subsequent annealing on Al-Ni multilayers. The evolution of the as-received laminated composite will be discussed in terms of the thickness reduction of the rolling process. More precisely, the question will be addressed whether the strain levels will affect the equilibrium between the various phases and their growth in the system.

2. Materials and Methods

The initial materials used in this investigation were commercially pure aluminum and nickel. Al and Ni strips were cut from as-received sheets, parallel to the original rolling direction. The chemical composition, the dimension of the strips and the mechanical properties of the as-received materials are

given in Table 1. The Ni strips were annealed at 610 °C for 30 min prior to processing, whereas the Al strips were processed in as-received condition so as to reduce the differences in hardness between the Al and Ni strips.

Table 1. Specifications of commercially pure Al and Ni sheets.

Material	Chemical Composition (wt %)	Strip Dimensions ($L \times W \times T$) (mm)	Yield Strength (MPa)	Tensile Strength (MPa)	Uniform Elongation (%)	Hardness (VHN)
Al (1100) As-received	99.11 Al, 0.17 Si, 0.49 Fe, 0.12Cu, 0.02 Mn, 0.09 others	100 mm × 74 mm × 2 mm	140.1	162.1	11.3	49
Ni (200 series) As-annealed	99.6 Ni, 0.3 Mn, 0.05 Si, 0.05 Fe	100 mm × 74 mm × 1 mm	220.6	560.4	8.9	109

Producing the initial sandwich requires the preparation of the surfaces of Al and Ni strips. Contaminations of greases, oxide films, moisture, and dust particles must be removed from the joined surfaces in order to produce clean surfaces. An acetone bath was employed to this purpose. After that, the clean surfaces were scratch brushed parallel to the rolling direction (RD) using a stainless steel brush with the wire diameter of 0.3 mm and a wire length of 60 mm. The brushed surfaces, due to increased roughness and removal of contamination, facilitate the cold joining during roll bonding. The roughness values of R_a were measured using surface roughness tester type Mitutoyo SJ-210 (Mitutoyo, Sakado, Japan) which were 3.9 µm for Ni and 3.5 µm for Al strips along the rolling direction. It is necessary to sandwich-roll the sheets immediately after brushing without touching the surfaces, in order to avoid oxide film formation and other disturbing factors. In this work, it was found that the allowed time interval between surface preparation and rolling should be less than 150 s.

According to the sketch in Figure 1, an initial sandwich with the dimensions of 100 (L//Rolling direction RD) × 74 (W//Transverse Direction TD) × 5 (T) mm^3 was formed by stacking two 2 mm thick Al sheets separated by a 1 mm thick Ni strip. Both ends of the stacked layers were fastened by steel wires. The sandwich was cold rolled in a rolling mill, with 220 mm diameter rolling cylinders and with 40 tons loading capacity and rolling speed of 300 rpm, without any lubricant.

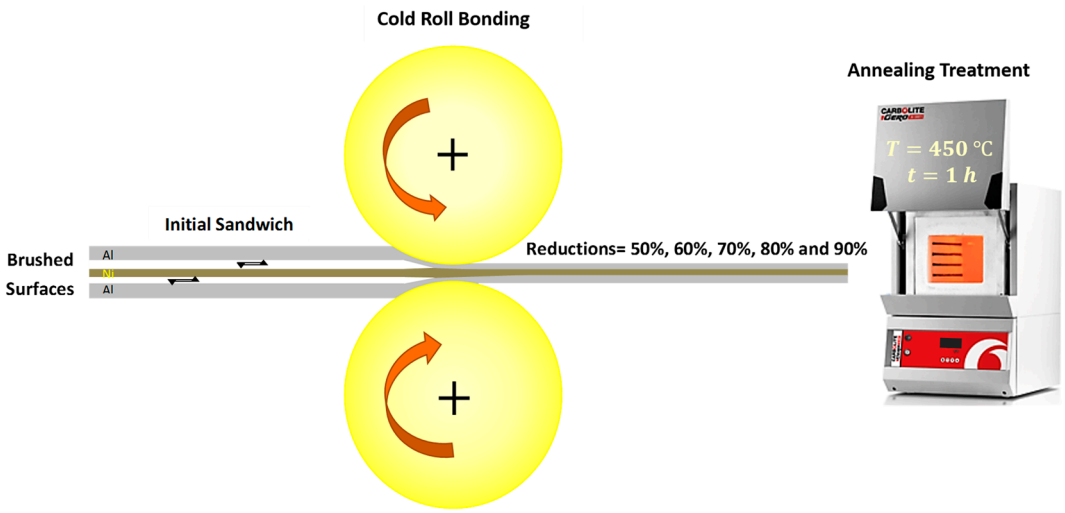

Figure 1. Schematic illustration of cold roll bonding and subsequent annealing processes for Al-Ni-Al sandwich stacked sample.

The CRB process was applied on the sandwich with five different thickness reductions of 50%, 60%, 70%, 80%, and 90% in 1, 2, 3, 4 and 5 passes, respectively, corresponding to respective true strains of 0.8, 1.06, 1.39, 1.86 and 2.66. It was observed that the bonding of stacked layers was not successful

with reductions of less than 50%. Corresponding to the applied reductions, the samples were labeled R_{50}, R_{60}, R_{70}, R_{80}, and R_{90}, respectively. Table 2 shows the reductions and corresponding thicknesses of the sandwich in each rolling pass.

Table 2. Applied reductions on sandwich (r_i) and its related thicknesses (x_i) (i is the number of rolling pass).

i	1	2	3	4	5
r_i (%)	50	60	70	80	90
x_i (mm)	2.5	2.0	1.5	1.0	0.5

After the CRB process, samples had the dimensions of 15 mm (L) × 10 mm (W). These specimens were annealed in a heat treatment furnace at 450 °C for 60 min. To avoid oxidation, samples were covered with alumina powders. In this step, the actual MIL-composites were formed as a result of diffusion processes. The schematic of the entire process (CRB and annealing) is illustrated in Figure 1.

Cross sections parallel to the RD-ND plane of as-annealed samples were prepared through standard metallography procedures. In order to investigate the microstructural evolution, a Philips XL30 scanning electron microscope (SEM, SEMTech Solutions, Inc., North Billerica, MA, USA) equipped with an energy dispersive spectrometer (EDS, Seron Technologies Inc., Gyeonggi-do, Korea) of type Seron AIS 2300® was used in addition to conventional optical microscopy (OM, Olympus Co., Shinjuku-Tokyo, Japan). Phase formation and chemical composition changes across the Al/Ni interfaces were studied by collecting point and line scans. The thickness of the continuous or segmented layers of the intermetallic phase was determined at several points of the formed layers using image analysis software (ImageJ2, ImageJ, 2009).

The composing phases of the MIL-composites were determined by X-ray diffraction (XRD, PANalytical B.V., Almelo, The Netherlands). A Philips X'pert MPD® diffractometer with Cu-Kα radiation (λ = 0.1542 nm) was used and XRD measurements were carried out at room temperature between $15° \leq 2\theta \leq 105°$, whereby X'pert HighScore plus® post processing software (2.2.2, PANalytical B.V., Almelo, The Netherlands, 2006) was employed to analyze the diffractograms.

3. Results and Discussion

3.1. Microstructure Evolution

Figure 2 shows the backscatter contrast images of the Al-Ni laminated composites, which were fabricated by the CRB process with 50%, 60%, 70%, 80%, and 90% reductions and subsequent annealing at 450 °C for 60 min. It can be seen that a new phase has formed at the Al/Ni interface. The micrographs of Figure 2a–e exhibit that the phase formation is affected by the level of strain. As can be observed in Figure 2a,f, 50% thickness reduction resulted in only some scarce nuclei of the new phase. However, 90% reduction resulted in a complete layer of intermetallic phase(s) (Figure 2e,j). The nucleation of the new phase at the interface of Al and Ni appears to indicate that a threshold strain for nucleation of approximately 50% reduction is required. Increased rolling reduction involves increased plastic strain, and causes the formation of an interface phase with the morphology of a continuous layer. Higher strain level results in increased defect density, especially sub-boundaries in metals with high stacking fault energy [35]. These high-energy defects are preferred sites for intermetallic phase nucleation, and thus, the nucleation rate increases with the increasing of strain. As a result, the phase nuclei coalesce during growth causing a continuous and homogenous layer after annealing of sample R_{90}.

Figure 2b,g show that after 60% reduction (sample R_{60}), the intermetallic layer has grown along the interface and extended to the Al and Ni lattices by atomic cross-interface diffusion. Additional to the higher density of crystallographic defects in sample R_{60}, the stronger bond strength reduces the diffusion barrier and hence facilitates nucleation of the new phase much more frequent than in the R_{50} sample. Similar observations can be made for samples R_{70}, R_{80}, R_{90}. Pipe diffusion processes

and increased bond strength promoted interdiffusion of Al and Ni atoms in R_{60}, R_{70}, and R_{80}, which resulted in the expansion and elongation of the layers. Finally, the merging of individual layer segments has produced a continuous layer in sample R_{90}.

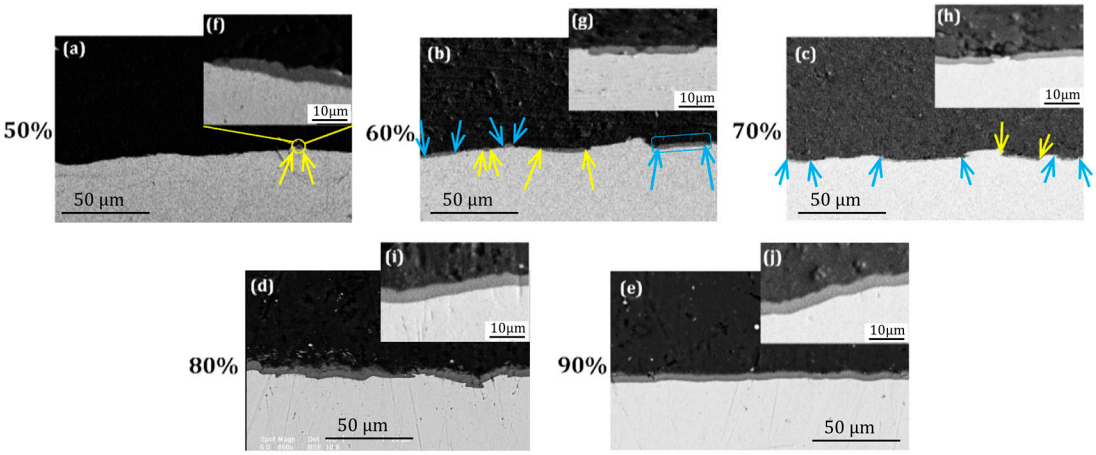

Figure 2. Backscattered electron (BSE) images of the microstructure of the Al/Ni interface, observed in the TD plane, of samples after reductions of 50% (**a**,**f**), 60% (**b**,**g**), 70% (**c**,**h**), 80% (**d**,**i**) and 90% (**e**,**j**), followed by annealing at 450 °C for 60 min. The colored arrows indicate intermetallic layer segments.

The possible occurrence of (partial) recrystallization in the Al and Ni substrates during annealing, may have removed part of the deformation sub-structures and hence may have affected the diffusion mechanisms occurring at the interface. The clarification of the possible effect of recrystallization and grain growth on diffusion processes needs a detailed investigation which has not been addressed in this work.

3.2. X-ray Diffraction Patterns

Figure 3 shows the XRD patterns measured on a slightly tilted cross-section of the rolled and annealed composite samples R_{50} and R_{90} (cf. Figure 3a), so that the plane of observation included both Al and Ni layers of the laminated composite. Not a single peak related to the Al-Ni intermetallic phase was identified in the R_{50} sample, cf. Figure 3b. This is presumably due to the fact that the volume fraction of the intermetallic compound was insufficient, although minute amounts of an intermetallic phase can be observed on the microstructural images (Figure 2a,f). In sample R_{90}, the peaks of Al, Ni, and Al_3Ni phases were well identified, cf. Figure 3c. This intermetallic compound formed as a thin layer of 4.1 µm average thickness at the interface of the Al and the Ni laminates (Figure 2e).

The Ni peaks in R_{90} were more intense than those in R_{50}, which can be explained in the following manner. In order to better expose the Al/Ni interface to the X-ray radiation, samples were mechanically polished in order to remove some of the Al layer from one side, cf. Figure 3a. This removal of the Al layer in R_{90} sample was more effective than in the R_{50} sample.

The XRD results were also confirmed by the EDS elemental analysis. On all samples, the compositional analysis of the intermetallic phase was performed along a line perpendicular to the interface. The results reveal that the elemental composition of the formed layers is identical, and only one kind of Al-Ni intermetallic compound was formed, namely Al_3Ni, irrespective of the applied reduction.

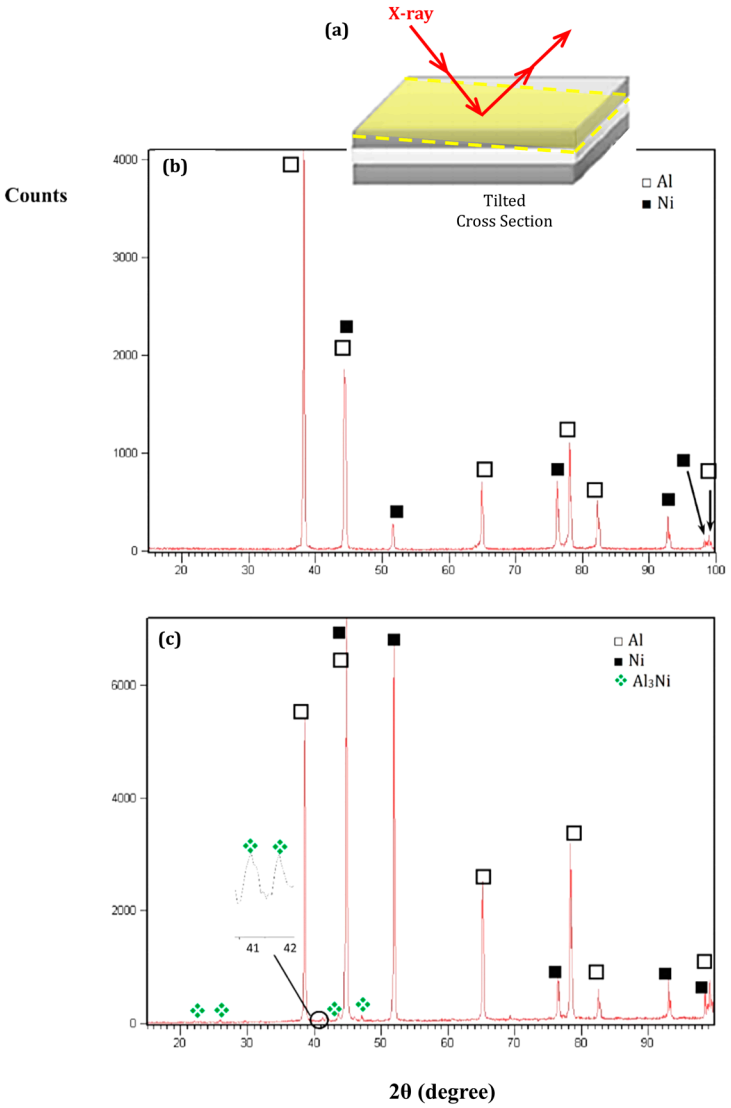

Figure 3. (**a**) Schematic representation of the tilted cross-section subjected to X-ray diffraction; X-ray diffraction patterns in (**b**) 50% and (**c**) 90% reduced samples, after cold roll bonding and subsequent annealing at 450 °C for 60 min. Only in 90% cold rolled sample the Al_3Ni intermetallic phase was identified, whereas in the 50% rolled sample the base metals Al and Ni were identified solely.

3.3. Phase Formation Mechanism: Phase Evolution during the Fabrication Process

An optical micrograph of the Al/Ni interface indicates that necking of the Ni layer has occurred in sample R_{90} after 90% reduction (Figure 4a). It is assumed that necking is a result of strain localization, which is a natural phenomenon occurring in the microstructure of rolled metals. Strain instabilities, which are very much likely to appear also in multi-layered materials, will give rise to local banding of the microstructure, producing e.g., deformation bands or shear bands, very well documented in single phase materials [31]. The initial roughness at the Al/Ni interface, induced by wire brushing of the sheet surface, may trigger such local irregularities of the strain field and give rise to the observed pattern of Ni necking.

On a somewhat smaller scale the interface exhibits a jagged character (Figure 4b), which is typical of layers in samples subjected to CRB. These observations confirm that according to the film theory [36] for scratch brushed surfaces, during the CRB process the Al and Ni layers could extrude through a fractured brittle Al_2O_3 oxide film and through the work-hardened layers. Subsequently, metallic bonded areas are formed, where opposing surfaces meet [37]. Moreover, interdiffusion of Al and Ni

may occur, though only over very short distances given the fact that there was no thermal activation as CRB was carried out at room temperature. Evidently, the clarification of this concept (i.e., whether or not such intermixed regions exist in the strips on which CRB was conducted or at the first stages of annealing) needs more detailed analysis. It could not be asserted here whether or not any solid solution area of base metals has formed during CRB. However, it has been understood that intermixing of components is a necessary initial process before the occurrence of any phase formation [27].

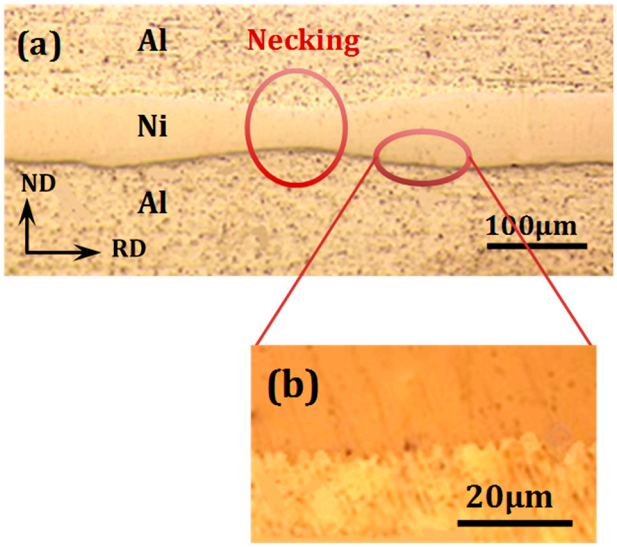

Figure 4. Optical micrographs observed on the TD section of the Al-Ni strip subjected to 90% reduction, before annealing; (**a**) necking of the Ni layer and (**b**) jagged Al/Ni interface.

Literature reports of the intermetallic formation mechanism in Al-Ni system emphasize on the composites, which were fabricated through ARB or F&R and subsequent annealing. It has been recognized that intermetallic phases are formed by nucleation and growth [7,24,27,33], which was concluded from differential scanning calorimetry (DSC) analysis [7,24,33], 3D atomic probe microscopy across the interface [27] and SEM micrographs [7]. In the ARB process, the intermixing of components occurred between multilayers during several cycles and it gave rise to the formation of an Al-Ni solid solution [27]. More rolling cycles gave rise to the development of a supersaturated solid solution [24]. Non-thermal diffusion, such as forced mixing or deformation-induced vacancies and dislocations, may promote intermixing of components at the nanoscale [27]. An intermetallic compound nucleates from this supersaturated solid solution after a short time of annealing at comparatively low temperature.

A simple calculation of the diffusion distance at room temperature shows that it is very unlikely to have observable diffusion of Ni in the Al sheet and vice versa. Even in the presence of a deformed matrix structure after (severe) rolling reduction, whereby the matrix material abounds in point and linear defects, it is still very unlikely that a measurable diffusion distance on the micrometer scale has occurred [27] in a roll bonded sample. The reason is that, on the one hand, the activation energy may have reduced because of the presence of a deformation (sub-) structure, but on the other hand it also may have increased because of the presence of a (partially) bonded interface, which imposes a diffusion barrier. Therefore, it can be ascertained that in the case under investigation intermetallic nucleation at room temperature did not occur, even not after a cold rolling reduction of 90% ($\bar{\varepsilon} = 2.66$), cf. Figure 4, which is in agreement with most studies on the formation of intermetallic phases during the CRB process after varying amounts of strain [2,7,18,27,38–40].

The above-mentioned mechanism of intermetallic phase formation implies that in the annealing step, an Al-Ni solid solution was formed before or even during the nucleation of intermetallic compounds. A redistribution of atoms is required to obtain the Al_3Ni stoichiometry [27,41], which only could occur at elevated temperatures during annealing. Ultimately, the intermetallic compound

was formed by nucleation and growth and an Al-Ni-based metal-intermetallic laminated composite was produced.

The Al-Ni phase diagram [42] is given in Figure 5a. It shows that the solubility of Ni in the Al lattice is negligible, whereas Al is considerably soluble in Ni with a solubility limit of 9 at % at 450 °C under equilibrium condition. Taking into account that the activation energy for the diffusion of Ni in Al (Q (Ni $\rightarrow$ Al) $\approx$ 66 kJ/mol [43]) is lower than the activation energy of Al in Ni (Q (Al $\rightarrow$ Ni) $\approx$ 90 kJ/mol [44]) at 450 °C, it is logical to assume that the diffusion distance of Ni in Al is larger than vice versa, and given the limited solubility of Ni in the Al lattice it would imply that the first intermetallic phase appears at the Ni/Al interface (cf. Figure 2) on the side of the Al layer, and at the Ni side of the interface a solid solution of Al in Ni should exist.

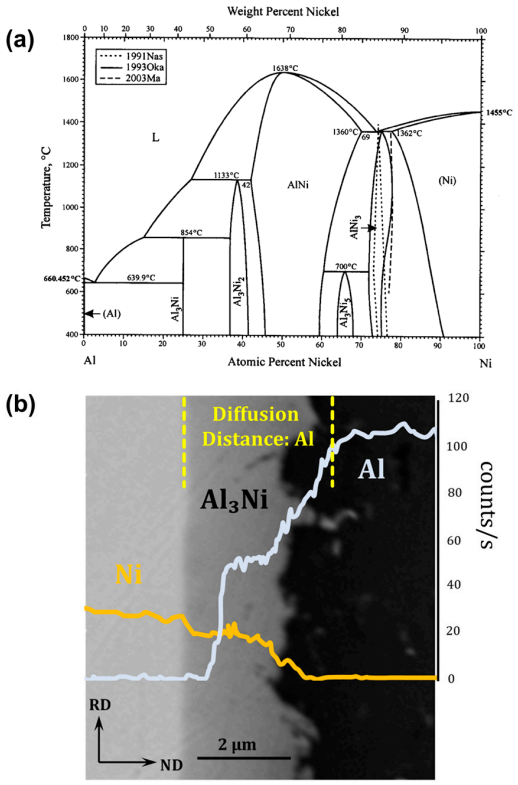

Figure 5. (**a**) The Al-Ni phase diagram [42], (**b**) typical energy dispersive spectrometry line profile of Al and Ni across the interface, observed in the RD-ND plane after 70% cold roll bonding and annealing at 450 °C for 60 min.

3.4. Atomic Diffusivity Observations

Concentration gradients of Al and Ni atoms at the Al/Ni interface were obtained from compositional line scans across the interface such as the one presented in Figure 5b. The intermetallic phase formation is a diffusion-controlled process. Diffusion of Al and Ni atoms before and during the nucleation of the Al_3Ni compound caused the concentration gradient of constituent atoms across the original Al/Ni interface. As a result, Al_3Ni or a mixture of Al_3Ni and Al solid solution in Ni were formed. It was reported [24,27,29,45–47] that the manufacturing process parameters, such as the build-up of the stacked sandwich sample, the strain levels, and ensuing defect concentration, alter the phase formation sequence and their growth kinetics. Although further verification is required to clarify the effect of these parameters in a comprehensive manner, a large number of reports have confirmed that the first kinetically favored intermetallic phase is the Al_3Ni compound. A number of these reports investigated the interface regions on either nanometer or micrometer scale.

Atomic diffusion distances, estimated from the EDS line scans, of Ni and Al versus thickness reduction are given in Figure 6a. The results show that the diffusion distances of Al (x_{Al}) and Ni (x_{Ni}) increased with the increasing reduction up to 80%, but decreased after 90% reduction. The higher reduction of 90% reduces the interface barrier activation energy of diffusion, which gives rise to rapid interdiffusion of atoms and the formation of Al → Ni solid solution at early annealing time. Subsequently, thermal energy and rest stored energy in cold-worked constituent layers supply the activation energy of Al_3Ni nucleation at much shorter annealing times in comparison with the material rolled to a reduction of 80% and lower. The nucleation of Al_3Ni from solid solution occurs simultaneously with interdiffusion of atoms into the opposite lattice. As the diffusion barrier in sample R_{90} is lower than in sample R_{80}, because of the better and more homogeneous bonding strength, a continuous intermetallic layer can be formed more readily in sample R_{90}. As diffusion of the component atoms through the compact intermetallic layer is slower and more difficult than diffusion through the opposite base metal lattice, it explains the reduced diffusion distances in sample R_{90} as compared to sample R_{80}. In sample R_{80} the intermetallic layer is segmented and leaves open gates for inter-diffusion of Ni and Al, explaining the larger diffusion distances. This is schematically proposed in Figure 6b, which shows the formation of solid solution and the Al_3Ni phase in samples R_{80} and R_{90} at the same annealing time. It can be said that the diffusion distance is the result of two opposing tendencies: (i) the activation energy imposed by the interface barrier, which reduces with increased rolling reduction (cf. Figure 6b) and (ii) the activation energy imposed by the newly formed intermetallic layer itself, which increases with increased rolling reduction.

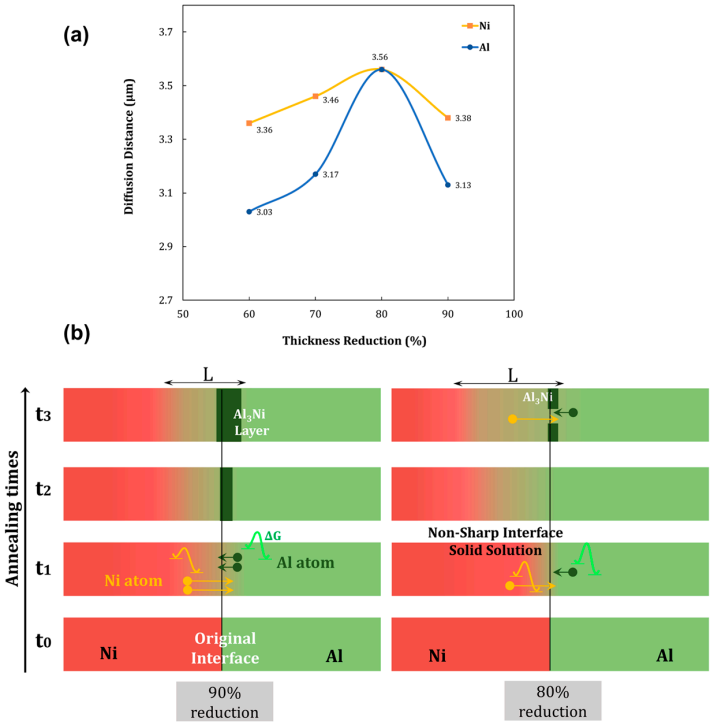

Figure 6. (**a**) Variation of Al and Ni diffusion distances across the Al/Ni interface versus cold rolling reduction after annealing at 450 °C for 60 min, (**b**) schematic representation of the Al/Ni interface in samples R_{90} and R_{80} at annealing times of t_0, t_1, t_2, and t_3; the Al_3Ni layer was formed at shorter annealing times in R_{90} and acted as a diffusion barrier, while a larger solid solution zone L has formed in R_{80}.

It is also clear that x_{Ni} is larger than x_{Al} for all reductions because Ni atoms are more mobile in aluminum than Al atoms in nickel, which is proved by the diffusion coefficient values of Ni in Al, 5.2×10^{-13} $(\frac{cm^2}{s})$, and Al in Ni, 5.9×10^{-16} $(\frac{cm^2}{s})$ at 450 °C [27,28,43,44].

3.5. Strain Effects on the Growth of the Intermetallic Compound

Figure 7 shows the effect of different reduction levels from 60% to 90% on the thickness of the formed intermetallic layer in Al-Al_3Ni-Ni composites. Because of the absence of an intermetallic layer in the 50% cold rolled sample, the layer thickness is not defined for that sample. The general trend of the intermetallic layer thickness is increasing and shows how the layer grows. In this respect, it was found that growth of the Al-rich intermetallic layer was a two-stage process [24] that can be described by the model of Coffey et al. [48]. The first stage was revealed as a stage of lateral growth along the interface until a continuous layer was created by coalescing of the discrete segments. The second stage involves thickening of the connected layers in the direction perpendicular to the interface. Actually, the growth mode changes from an interface-controlled stage, followed by the second stage in which bulk diffusion-controlled growth occurs.

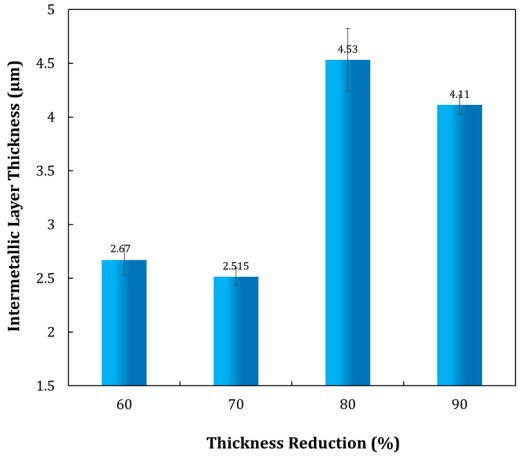

Figure 7. Intermetallic layer thickness dependence versus cold roll bonding reduction after annealing at 450 °C for 60 min.

3.6. The Morphology of Interfaces in the Metal-Intermetallic Laminate Composite

The driving force for the formation of intermetallic phases is given by the reduction of Gibbs free energy, whereas the activation energy barrier is composed of two components: (i) the activation energy for bulk diffusion of Ni in Al and vice versa and (ii) the incomplete bonding at the Ni/Al interface, particularly at the lower reductions, which may impose an effective barrier for diffusion across the interface.

Figure 8 shows the Al-Al_3Ni-Ni laminated composite micrographs in the annealed R_{80} sample. The micrographs exhibit wrinkled (Figure 8a) and discontinuous (Figure 8b) interfaces. The wrinkled interfaces (also cf. Figure 2d,e) originate from the jagged interfaces with increased roughness and work-hardening induced by severe wire brushing of the metal surface (cf. Figure 4), which is probably responsible for mechanical bonding during the CRB step and of which the complicated intricate morphology also may affect the formation of the new interface between the base metals and Al_3Ni phase during annealing.

It also can be observed on the micrograph of Figure 8b that the discontinuous intermetallic interface exhibits, at some locations, Ni streaks extending to the Al side of the interface. The Ni streaks appearing at the interface could be explained by the following mechanism. It is reasonable to assume that thermal-stress cracks may appear in the brittle Al_3Ni layer, because of local thermal gradients and the different thermal expansion coefficients of the brittle intermetallic and Al or Ni base layers. Diffusion of constituents through these cracks, most noticeably the diffusion of Ni (because of its higher diffusion coefficient) may fill up these cracks with Ni. The Ni-filled pattern of cracks may circumvent certain segments of the intermetallic interface, eventually giving rise to the formation of

isolated Al_3Ni islands in the Al ductile matrix. The various sequences of this mechanism are shown in the schematic representation of Figure 9.

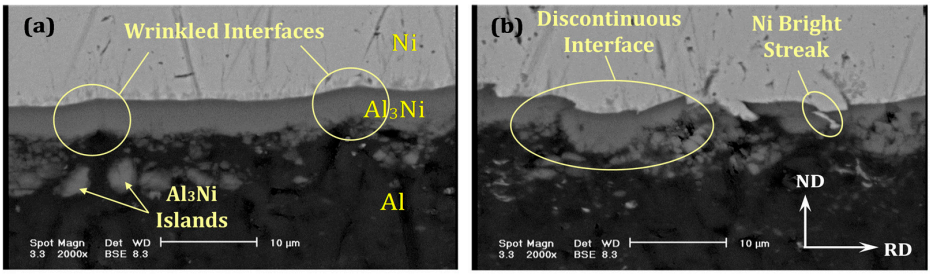

Figure 8. BSE images observed on the TD section of the 80% cold rolled and annealed sample; (**a**) wrinkled and (**b**) discontinuous interface. In (**b**) bright streaks are observed of pure Ni diffusion through thermal stress cracks of the brittle Al_3Ni intermetallic layer.

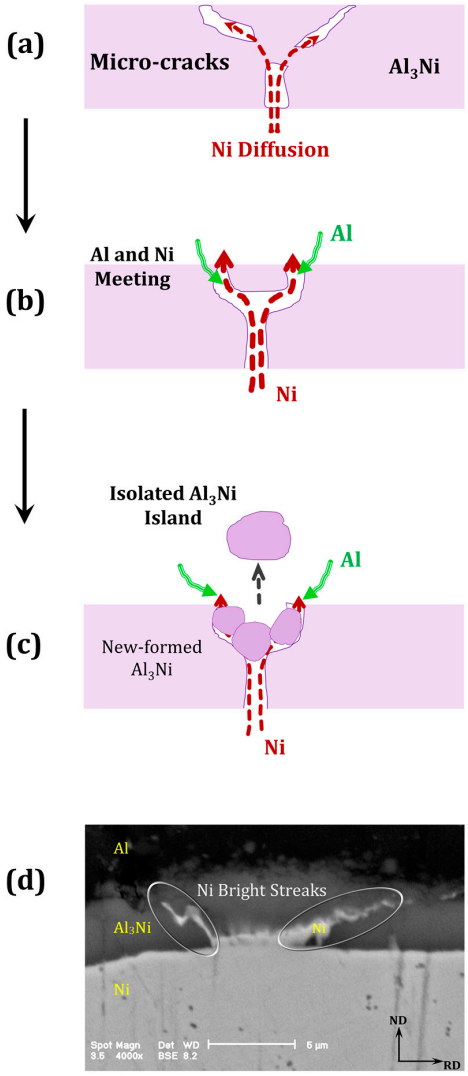

Figure 9. Schematic representation of the subsequent stages in the formation mechanism of Al_3Ni islands; (**a**) Ni diffusion through cracks in brittle Al_3Ni layer; (**b**) coarsening and merging of cracks; (**c**) Isolation and separation of Al_3Ni phase under driving pressure of Ni diffusion, (**d**) BSE image of bright Ni streaks diffusing through thermal stress cracks of Al_3Ni layer in sample R_{90}.

4. Conclusions

In this investigation, an Al-Al_3Ni-Ni laminated composite was produced through a process of cold roll bonding of an Al/Ni/Al stacked sandwich sample and subsequent annealing. The way in which applied strain has affected the formation of intermetallic phases was studied and a number of conclusions could be derived. A layer of Al_3Ni is formed at the cold bonded interface of the Al and Ni sheet, when a rolling reduction is applied with a reduction of 50% to 90% and following an annealing treatment of 60 min at 450 °C. With the lower reductions of 60% and 70% a highly-segmented layer was formed, which has modified to a continuous layer of 4.1 µm thickness after 90% reduction. It was surmised that the incomplete bonding of the Ni/Al interface at the lower reduction imposed a diffusion barrier and therefore the Al_3Ni layer only could form in a segmented manner. It was also observed that the Al_3Ni intermetallic layer was primarily formed at the Al side of the initial Al/Ni interface, because of the higher diffusivity of Ni in the Al lattice and the near to zero solubility of Ni in Al. Irrespective of the applied rolling reduction the Al_3Ni intermetallic layer was exclusively observed, without the presence of any other intermetallic phase. The Al/Al_3Ni and Ni/Al_3Ni interfaces exhibited a wrinkled morphology, which was the result of the initial roughness and work-hardening of the wire-brushed sheet surface and the mechanical type bonding occurring during cold rolling. At some locations at the interface Al_3Ni isolated islands were formed, for which a presumed formation mechanism was presented in the present paper.

Author Contributions: All the authors contributed to the present work. Monireh Azimi designed and performed experiments, analyzed data and wrote the paper; Mohammad Reza Toroghinejad designed experiments and gave technical and conceptual advice; Morteza Shamanian commented on data analyses; Leo A. I. Kestens gave conceptual advice and wrote the paper; all authors discussed the results and implications and commented on the manuscript at all stages.

Conflicts of Interest: The authors declare no conflict of interest.

References

1. Konieczny, M. Microstructural characterisation and mechanical response of laminated Ni-intermetallic composites synthesised using Ni sheets and Al foils. *Mater. Charact.* **2012**, *70*, 117–124. [CrossRef]
2. Srivastava, V.C.; Singh, T.; Chowdhury, S.G.; Jindal, V. Microstructural characteristics of accumulative roll-bonded Ni-Al-based metal-intermetallic laminate composite. *J. Mater. Eng. Perform.* **2012**, *21*, 1912–1918. [CrossRef]
3. Tixier, S.; Böni, P.; van Swygenhoven, H. Hardness enhancement of sputtered Ni3Al/Ni multilayers. *Thin Solid Films* **1999**, *342*, 188–193. [CrossRef]
4. Anderson, P.M.; Bingert, J.F.; Misra, A.; Hirth, J.P. Rolling textures in nanoscale Cu/Nb multilayers. *Acta Mater.* **2003**, *51*, 6059–6075. [CrossRef]
5. Misra, A.; Demkowicz, M.J.; Zhang, X.; Hoagland, R.G. The radiation damage tolerance of ultra-high strength nanolayered composites. *JOM J. Miner. Met. Mater. Soc.* **2007**, *59*, 62–65. [CrossRef]
6. Kaneko, Y.; Sakakibara, H.; Hashimoto, S. Microstructure and Vickers hardness of Co/Cu multilayers fabricated by electrodeposition. *J. Mater. Sci.* **2008**, *43*, 3931–3937. [CrossRef]
7. Mozaffari, A.; Hosseini, M.; Manesh, H.D. Al/Ni metal intermetallic composite produced by accumulative roll bonding and reaction annealing. *J. Alloys Compd.* **2011**, *509*, 9938–9945. [CrossRef]
8. Harach, D.; Vecchio, K. Microstructure evolution in metal-intermetallic laminate (MIL) composites synthesized by reactive foil sintering in air. *Metall. Mater. Trans. A* **2001**, *32*, 1493–1505. [CrossRef]
9. Hoseini-Athar, M.M.; Tolaminejad, B. Interface morphology and mechanical properties of Al-Cu-Al laminated composites fabricated by explosive welding and subsequent rolling process. *Met. Mater. Int.* **2016**, *22*, 670–680. [CrossRef]
10. Jindal, V.; Srivastava, V.C.; Das, A.; Ghosh, R.N. Reactive diffusion in the roll bonded iron—Aluminum system. *Mater. Lett.* **2006**, *60*, 1758–1761. [CrossRef]
11. Jindal, V.; Srivastava, V.C.; Ghosh, R.N. Development of IF steel-Al multilayer composite by repetitive roll bonding and annealing process. *Mater. Sci. Technol.* **2008**, *24*, 798–802. [CrossRef]

12. Mizuuchi, K.; Inoue, K.; Sugioka, M.; Itami, M.; Lee, J.; Kawahara, M. Properties of Ni-aluminides-reinforced Ni-matrix laminates synthesized by pulsed-current hot pressing (PCHP). *Mater. Sci. Eng. A* **2006**, *428*, 169–174. [CrossRef]
13. Kim, H.Y.; Chung, D.S.; Hong, S.H. Reaction synthesis and microstructures of NiAl/Ni micro-laminated composites. *Mater. Sci. Eng. A* **2005**, *396*, 376–384. [CrossRef]
14. Kuk, S.W.; Yu, J.; Ryu, H.J. Effects of interfacial Al oxide layers: Control of reaction behavior in micrometer-scale Al/Ni multilayers. *Mater. Des.* **2015**, *84*, 372–377. [CrossRef]
15. Peng, L.M.; Wang, J.H.; Li, H.; Zhao, J.H.; He, L.H. Synthesis and microstructural characterization of Ti-Al_3Ti metal-intermetallic laminate (MIL) composites. *Scr. Mater.* **2005**, *52*, 243–248. [CrossRef]
16. Rohatgi, A.; Harach, D.J.; Vecchio, K.S.; Harvey, K.P. Resistance-curve and fracture behavior of Ti-Al_3Ti metallic-intermetallic laminate (MIL) composites. *Acta Mater.* **2003**, *51*, 2933–2957. [CrossRef]
17. Gurevich, L.; Pronichev, D.; Trunov, M. Structure Formation Mechanisms during Solid Ti with Molten Al Interaction. In *IOP Conference Series: Materials Science and Engineering, Proceedings of the International Conference on Advanced Materials and New Technologies in Modern Materials Science 2015, Tomsk, Russia, 9–11 November 2015*; IOP Publishing: Bristol, UK, 2016; Volume 116, pp. 12011–12020.
18. Yu, H.; Lu, C.; Tieu, A.K.; Li, H.; Godbole, A.; Kong, C. Annealing effect on microstructure and mechanical properties of Al/Ti/Al laminate sheets. *Mater. Sci. Eng. A* **2016**, *660*, 195–204. [CrossRef]
19. Peng, X.K.; Wuhrer, R.; Heness, G.; Yeung, W.Y. On the interface development and fracture behaviour of roll bonded copper/aluminium metal laminates. *J. Mater. Sci.* **1999**, *34*, 2029–2038. [CrossRef]
20. Li, X.; Zu, G.; Wang, P. Microstructural development and its effects on mechanical properties of Al/Cu laminated composite. *Trans. Nonferr. Met. Soc. China* **2015**, *25*, 36–45. [CrossRef]
21. Lee, T.; Sim, M.; Joo, S.; Park, K.; Jeong, H.; Lee, J. Effect of intermetallic compound thickness on anisotropy of Al/Cu honeycomb rods fabricated by hydrostatic extrusion process. *Trans. Nonferr. Met. Soc. China* **2016**, *26*, 456–463. [CrossRef]
22. Liu, C.Y.; Jing, R.; Wang, Q.; Zhang, B.; Jia, Y.Z.; Ma, M.Z.; Liu, R.P. Fabrication of Al/Al_3Mg_2 composite by vacuum annealing and accumulative roll-bonding process. *Mater. Sci. Eng. A* **2012**, *558*, 510–516. [CrossRef]
23. Liu, H.S.; Zhang, B.; Zhang, G.P. Microstructures and mechanical properties of Al/Mg alloy multilayered composites produced by accumulative roll bonding. *J. Mater. Sci. Technol.* **2011**, *27*, 15–21. [CrossRef]
24. Yang, D.; Hodgson, P.; Wen, C. The kinetics of two-stage formation of $TiAl_3$ in multilayered Ti/Al foils prepared by accumulative roll bonding. *Intermetallics* **2009**, *17*, 727–732. [CrossRef]
25. Desré, P.J.; Yavari, A.R. Suppression of crystal nucleation in amorphous layers with sharp concentration gradients. *Phys. Rev. Lett.* **1990**, *64*, 1533–1536. [CrossRef] [PubMed]
26. Tu, K.N.; GöSele, U. Effect of concentration gradient on phase stability. *MRS Online Proc. Libr. Arch.* **1982**, *19*, 375. [CrossRef]
27. Sauvage, X.; Dinda, G.P.; Wilde, G. Non-equilibrium intermixing and phase transformation in severely deformed Al/Ni multilayers. *Scr. Mater.* **2007**, *56*, 181–184. [CrossRef]
28. Colgan, E.G.; Mayer, J.W. Diffusion markers in Al/metal thin-film reactions. *Nucl. Inst. Methods Phys. Res. Sect. B Beam Interact. Mater. Atoms* **1986**, *17*, 242–249. [CrossRef]
29. Ma, E.; Nicolet, M.-A.; Nathan, M. $NiAl_3$ formation in Al/Ni thin-film bilayers with and without contamination. *J. Appl. Phys.* **1989**, *65*, 2703–2710. [CrossRef]
30. Jindal, V.; Srivastava, V.C. Growth of intermetallic layer at roll bonded IF-steel/aluminum interface. *J. Mater. Process. Technol.* **2008**, *5*, 88–93. [CrossRef]
31. Mozaffari, A.; Manesh, H.D.; Janghorban, K. Evaluation of mechanical properties and structure of multilayered Al/Ni composites produced by accumulative roll bonding (ARB) process. *J. Alloys Compd.* **2010**, *489*, 103–109. [CrossRef]
32. Battezzati, L.; Antonione, C.; Fracchia, F. Ni-Al intermetallics produced by cold-rolling elemental sheets. *Intermetallics* **1995**, *3*, 67–71. [CrossRef]
33. Battezzati, L.; Pappalepore, P.; Durbiano, F. Solid state reactions in Al/Ni alternate foils induced by cold rolling and annealing. *Acta Mater.* **1999**, *47*, 1901–1914. [CrossRef]
34. Brunelli, K.; Peruzzo, L. The effect of prolonged heat treatments on the microstructural evolution of Al/Ni intermetallic compounds in multi layered composites. *Mater. Chem. Phys.* **2015**, *150*, 350–358. [CrossRef]
35. Humphreys, F.J.; Hatherly, M. *Recrystallization and Related Annealing Phenomena*, 2nd ed.; Elsevier Ltd.: Oxford, UK, 2004.

36. Bay, N. Cold Welding Part 1: Characteristics, bonding mechanisms, bond strength. *Met. Constr.* **1986**, *18*, 369–372.
37. Mehr, V.Y.; Toroghinejad, M.R.; Rezaeian, A. The effects of oxide film and annealing treatment on the bond strength of Al-Cu strips in cold roll bonding process. *J. Mater.* **2014**, *53*, 174–181. [CrossRef]
38. Acoff, V.L.; Zhang, R.G. Processing Ti-Al-Nb Composite Sheet Materials Using Cold Roll Bonding and Reaction Annealing. In *Materials Science Forum*; Trans Tech Publications: Stafa-Zurich, Switzerland, 2007; Volume 539, pp. 791–796.
39. Hsieh, C.-C.; Shi, M.-S.; Wu, W. Growth of intermetallic phases in Al/Cu composites at various annealing temperatures during the ARB process. *Metals Mater. Int.* **2012**, *18*, 1–6. [CrossRef]
40. Zhang, R.; Acoff, V.L. Processing sheet materials by accumulative roll bonding and reaction annealing from Ti/Al/Nb elemental foils. *Mater. Sci. Eng. A* **2007**, *463*, 67–73. [CrossRef]
41. Wang, Q.W.; Fan, G.H.; Geng, L.; Zhang, J.; Zhang, Y.Z.; Cui, X.P. Formation of intermetallic compound layer in multi-laminated Ni-(TiB_2/Al) composite sheets during annealing treatment. *Micron* **2013**, *45*, 150–154. [CrossRef] [PubMed]
42. Okamoto, H. Al-Ni (Aluminum-Nickel). *J. Ph. Equilib. Diffus.* **2004**, *25*, 394. [CrossRef]
43. Hirano, K.; Agarwala, R.P.; Cohen, M. Diffusion of iron, nickel and cobalt in aluminum. *Acta Metall.* **1962**, *10*, 857–863. [CrossRef]
44. Hasaka, M.; Morimura, T.; Uchiyama, Y.; Kondo, S.I.; Watanabe, T.; Hisatsune, K.; Furuse, T. Diffusion of copper, aluminum and boron in nickel. *Scr. Metall. Mater.* **1993**, *29*, 959–962. [CrossRef]
45. Jeske, T.; Seibt, M.; Schmitz, G. Microstructural influence on the early stages of interreaction of Al/Ni-investigated by TAP and HREM. *Mater. Sci. Eng. A* **2003**, *353*, 105–111. [CrossRef]
46. Pretorius, R.; Marais, T.K.; Theron, C.C. Thin film compound phase formation sequence: An effective heat of formation model. *Mater. Sci. Rep.* **1993**, *10*, 1–83. [CrossRef]
47. Jeske, T.; Schmitz, G. Influence of the microstructure on the interreaction of Al/Ni investigated by tomographic atom probe. *Mater. Sci. Eng. A* **2002**, *327*, 101–108. [CrossRef]
48. Coffey, K.R.; Clevenger, L.A.; Barmak, K.; Rudman, D.A.; Thompson, C.V. Experimental evidence for nucleation during thin-film reactions. *Appl. Phys. Lett.* **1989**, *55*, 852. [CrossRef]